A Simple Kriging Method Incorporating Multiscale Measurements in Geochemical Survey

Changjiang Li[a] , Zhiming Lu[b], Tuhua Ma[a], Xingsheng Zhu[a]

[a]Zhejiang Information Center of Land and Resources,310007, Hangzhou,

People's Republic of China; email: zjigmr@mail.hz.zj.cn

[b]Hydrology and Geochemistry Group (EES-6), Los Alamos National Laboratory, Los Alamos,

NM 87545, USA: email: zhiming@lanl.gov

Corresponding Author:

C. Li

Zhejiang Information Center of Land and Resources,

310007, Hangzhou, People's Republic of China

Email: zjigmr@mail.hz.zj.cn

ABSTRACT

In this study, we propose a kriging algorithm, multiscale-kriging model, to incorporate geochemical data observed at multiscales (multi-resolutions). We assume that there are a number of measurements at different scales, and that the target scale at which the parameter values are needed may be different from the measurement scales. Several synthetic examples and the vanadium geochemical data from 8402 stream sediment samples in Zhejiang Province, China, have been used to illustrate the method. These examples demonstrate that, by incorporating measurements from all scales, the estimated field is better than the field estimated using measurements from any individual scale. This method also allows us to estimate a parameter field at the scale that does not have any measurements.

KEYWORDS: **kriging, simple multiscale-kriging, multiresolution data, geochemical survey**

Introduction

Kriging has been widely used in geosciences to incorporate spatially sampled data and to estimate the conditional mean field and its associated (co-)variance [*Journel and Huijbregts*, 1978; *Clark*, 1979; *Kitanidis*, 1997; *Deutsch and Journel*, 1998; *Zhao*, 2004]. Although in many applications, such as geochemical mapping in a region, samples may be taken at different scales (resolutions) in various cycles of geological surveys, quite often these scales are different from the scale at which estimates are needed. In other words, we need a methodology to incorporate spatially sampled data with different resolutions and obtain the reasonable parameter values at a desired scale. Few studies investigated the effect of multiscale data on the estimated field. *Kupfersberger* et al. (1998) studied multiscale cokriging with a primary attribute and a second attribute, where the second attribute is available at a large scale and the primary attribute is measured at the modeling scale. The measurements of the second attribute at large scale are used to improve the estimate of the primary attribute.

In this research, we assume that the parameter of interest is measured at several different scales (resolutions). Our aim is to estimate the conditional mean field and conditional covariance of the parameter at a target scale, which may be different from measurement scales. In addition, measurements may or may not be available at this target scale.

The paper is organized as follow. In section 2, we first formulate the kriging estimate using all measurements at different scales. The covariance functions across different scales, which are required in solving the kriging system, are given in Section 3. The applicability of the proposed method is then demonstrated in Section 4, using several synthetic examples and

a set of vanadium geochemical data measured from 8402 stream sediment samples, followed by a short summary.

Multiscale Simple Kriging

Let Y be a second-order stationary random function defined on domain Ω, characterized by the mean $\langle Y \rangle$ and the unconditional covariance function $C_Y(\mathbf{x}, \mathbf{y})$, for $\mathbf{x}$, $\mathbf{y} \in \Omega$. Suppose that we have observed $Y(\mathbf{x})$ at K different scales (resolutions) S_1, S_2, $\cdots$, S_K, and that there are N_k measurements at scale S_k, observed at locations $\mathbf{x}_i^{(k)}$, $i = \overline{1, N_k}$ and $k = \overline{1, K}$. For any $\mathbf{x}$ at the scale S_0, which may be different from any observation scale S_k, $k = \overline{1, K}$, the kriging estimation may be written as a linear combination of all available measurements,

$$Y^{(0)}(\mathbf{x}) = \sum_{k=1}^{K} \sum_{i=1}^{N_k} \alpha_i^{(k)}(\mathbf{x}) Y^{(k)}(\mathbf{x}_i^{(k)}), \tag{1}$$

where coefficients $\alpha_i^{(k)}(\mathbf{x})$ are determined by minimizing the estimate errors at the ensemble sense, which yields the kriging equations

$$\sum_{k=1}^{K} \sum_{i=1}^{N_k} \alpha_i^{(k)}(\mathbf{x}) C_Y^{(k,n)}(\mathbf{x}_i^{(k)}, \mathbf{x}_j^{(n)}) = C_Y^{(o,n)}(\mathbf{x}, \mathbf{x}_j^{(n)}), \quad n = \overline{1, K}, j = \overline{1, N_n} \tag{2}$$

where $C_Y^{(k,n)}$ is the covariance function between scales S_k and S_n, and $C_Y^{(0,n)}$ is coverance between scales S_n and S_0, which is the scale of being estimated. There are $N = \sum_{k=1}^{K} N_k$ linear equations and N unknowns in Equation (2). Note that coefficients $\alpha_i^{(k)}$ are location-dependent, which means that the set of linear algebraic equations in Equation (2) have to be solved for each location of interest at scale S_0.

The conditional covariance at scale S_0 can be derived as

$$^{(c)}C_Y^{(0)}(\mathbf{x}, \mathbf{y}) = C_Y^{(0)}(\mathbf{x}, \mathbf{y}) - \sum_{k=1}^{K} \sum_{i=1}^{N_k} \alpha_i^{(k)}(\mathbf{x}) C_Y^{(0,k)}(\mathbf{y}, \mathbf{x}_i^{(k)}), \tag{3}$$

where $C_Y^{(0)}(\mathbf{x}, \mathbf{y})$ is the unconditional covariance between $\mathbf{x}$ and $\mathbf{y}$ at scale S_0, which in general is different from the unconditional covariance at other scales. The critical issue in this multiscale kriging method is how to find covariance functions within any scale and between different scales, which will be elaborated in the next section.

Determination of Covariance between Different Scales

For convenience of presentation, we start from the one-dimensional problem. Given a second-order stationary random field $Y(x)$, where x is a point in domain Ω, we consider an averaged quantity of $Y(x)$ over a segment of length T centered at x,

$$Y_T(x) = \frac{1}{T} \int_{x-T/2}^{x+T/2} Y(u) du. \tag{4}$$

Since Y is a spatially random variable, and so is the averaged quantity Y_T. It is seen from the equation that Y_T has the same mean as the original variable Y, i.e., $\langle Y_T(x) \rangle = \langle Y(x) \rangle$. From Equation (4), one can derive the perturbation term as

$$Y_T'(x) = \frac{1}{T} \int_{x-T/2}^{x+T/2} Y'(u) du. \tag{5}$$

where Y' stands for the perturbation of the original random variable Y. From this equation, it can be shown that the variance of Y_T is different from that of Y and can be written as $var(Y_T(x)) = \sigma_Y^2 \gamma(T)$, where σ_Y^2 is the variance of Y and $\gamma(T)$ is called the variance function [*Vanmarcke*,1983]. The variance function $\gamma(T)$ measures the reduction of the point variance under local averaging and may be found as

$$\gamma(T) = \frac{1}{T^2} \int_0^T \int_0^T \rho(x_1 - x_2) dx_1 dx_2 = \frac{2}{T} \int_0^T \left(1 - \frac{\tau}{T} \right) \rho(\tau) d\tau. \tag{6}$$

where ρ is the correlation function of $Y(x)$. The variance function satisfies $\gamma(T) \geq 0$, $\gamma(0) = 1$, and $\gamma(-T) = \gamma(T)$. Note that for a stationary field $Y(x)$, $Y_T(x)$ is also stationary. For a general form of covariance function $\rho(\tau)$, $\gamma(T)$ in Equation (6) should be evaluated numerically. However, for some special correlation functions, $\gamma(T)$ can be derived

analytically. For example, for an exponential correlation function $\rho(\tau) = \exp(-|\tau|/\lambda)$, where λ is the correlation length of $Y(x)$, we have

$$\gamma(T) = \gamma_1^e(T,\lambda) = 2\left(\frac{\lambda}{T}\right)^2\left[\frac{T}{\lambda} - 1 + e^{-T/\lambda}\right], \tag{7}$$

and for a Gaussian correlation function $\rho(\tau) = \exp(-\tau^2/\lambda^2)$,

$$\gamma(T) = \gamma_1^g(T,\lambda) = \left(\frac{\lambda}{T}\right)^2\left(\sqrt{\pi}\frac{T}{\lambda}E(T/\lambda) + e^{-T^2/\lambda^2} - 1\right), \tag{8}$$

where E is the error function. Subscript "1" in Equations (7) and (8) denotes variance functions for one-dimensional problems, and superscripts "e" and "g" stands for exponential and Gaussian covariance functions, respectively. Note that $\gamma(T)$ satisfies $\lim_{T\to\infty}\gamma(T) = 0$ for all these cases, which is the condition for ergodicity in the mean.

The covariance between two averaged random variables Y_T and $Y_{T'}$, where T and T' are two segments in the domain and may represent two different resolutions, can be expressed as [*Vanmarcke*, 1983]

$$cov(Y_T, Y_{T'}) = \frac{\sigma_Y^2}{2TT'}\sum_{k=0}^{3}(-1)^k T_k^2 \gamma(T_k), \tag{9}$$

where T_k are defined in Figure 1. Although this figure depicts a special case in which T and T' are partially overlapping, Equation (9) is valid no matter whether they are overlapping or not. For a given correlation function ρ, once the variance function γ is found, one can compute $cov(Y_T, Y_{Y'})$ from Equation (9).

The above derivations can be easily extended to two-dimensional random fields. The local average of a field $Y(\mathbf{x})$, where $\mathbf{x} = (x_1, x_2)$, over a rectangular block A centered at $\mathbf{x}$ is defined as

$$Y_A(\mathbf{x}) = \frac{1}{|A|}\int_A Y(\mathbf{y})d\mathbf{y}, \tag{10}$$

where $|A|$ denotes the area of the block A. The covariance function between any two blocks

A and A', which can be considered as two different resolutions, can be written as [*Vanmarcke*, 1983]

$$cov(Y_A, Y_{A'}) = \frac{\sigma_Y^2}{4|A||A'|} \sum_{k=0}^{3} \sum_{m=0}^{3} (-1)^{k+m} T_{1k}^2 T_{2m}^2 \gamma(T_{1k}, T_{2m}) \qquad (11)$$

where T_{1k} and T_{2m} are defined in Figure 2 and the variance function γ is given as

$$\gamma(T_{1k}, T_{2m}) = \frac{4}{T_{1k} T_{2m}} \int_0^{T_{1k}} \int_0^{T_{2m}} \left(1 - \frac{\tau_1}{T_{1k}}\right)\left(1 - \frac{\tau_2}{T_{2m}}\right) \rho(\tau_1, \tau_2) d\tau_1 d\tau_2. \qquad (12)$$

In particular, if the covariance of $Y(\mathbf{x})$ is an exponential correlation function $\rho(\tau_1, \tau_2) = \exp(-|\tau_1|/\lambda_1 - |\tau_2|/\lambda_2)$, where λ_1 and λ_2 are the correlation lengths in x_1 and x_2 directions, respectively, one has $\gamma(T_{1k}, T_{2m}) = \gamma_1^e(T_{1k}, \lambda_1)\gamma_1^e(T_{2m}, \lambda_2)$, and for an Gaussian correlation function $\rho(\tau_1, \tau_2) = \exp(-\tau_1^2/\lambda_1^2 - \tau_2^2/\lambda_2^2)$, $\gamma(T_{1k}, T_{2m}) = \gamma_1^g(T_{1k}, \lambda_1)\gamma_1^g(T_{2m}, \lambda_2)$.

Similarly, for three-dimensional problems, the local average of the random field $Y(\mathbf{x})$ is defined as

$$Y_V(\mathbf{x}) = \frac{1}{|V|} \int_V Y(\mathbf{y}) d\mathbf{y}, \qquad (13)$$

where V is the block centered at $\mathbf{x}$ and $|V|$ is the volume of the block. The covariance between two blocks V and V' can be expressed as

$$cov(Y_V(\mathbf{x}), Y_{V'}(\mathbf{x}')) = \frac{\sigma_Y^2}{8|V||V'|} \sum_{k=0}^{3} \sum_{m=0}^{3} \sum_{n=0}^{3} (-1)^{k+m+n} T_{1k}^2 T_{2m}^2 T_{3n}^2 \gamma(T_{1k}, T_{2m}, T_{3n}), \qquad (14)$$

where $|V|$ and $|V'|$ stand for the volume of blocks V and V', and T_{1k} and T_{2m}, $k, m = 1, 2, 3$, are various lengths defined similarly as in the two-dimensional case, and the variance function γ is given as

$$\gamma(T_{1k}, T_{2m}, T_{3n}) = \frac{8}{T_{1k} T_{2m} T_{3n}} \int_0^{T_{1k}} \int_0^{T_{2m}} \int_0^{T_{3n}} \left(1 - \frac{\tau_1}{T_{1k}}\right)\left(1 - \frac{\tau_2}{T_{2m}}\right)\left(1 - \frac{\tau_3}{T_{3n}}\right)$$

$$\rho(\tau_1, \tau_2, \tau_3) d\tau_1 d\tau_2 d\tau_3. \qquad (15)$$

If the covariance function is exponential correlation function $\rho(\tau_1, \tau_2, \tau_3) =$

$\exp(-|\tau_1|/\lambda_1-|\tau_2|/\lambda_2-|\tau_3|/\lambda_3)$, $\gamma(T_{1k},T_{2m},T_{3n})=\gamma_1^e(T_{1k},\lambda_1)\gamma_1^e(T_{2m},\lambda_2)\gamma_1^e(T_{1n},\lambda_3)$, and for

the Gaussian correlation function $\rho(\tau_1,\tau_2,\tau_3)=\exp(-\tau_1^2/\lambda_1^2-\tau_2^2/\lambda_2^2-\tau_3^2/\lambda_3^2)$,

$\gamma(T_{1k},T_{2m},T_{3n})=\gamma_1^g(T_{1k},\lambda_1)\gamma_1^g(T_{2m},\lambda_2)\gamma_1^g(T_{2n},\lambda_3)$.

It should be noted that the above derivations can be easily extended to the case with

space-dependent mean field. In this case, ordinary kriging rather than the simple kriging

should be used. Finally, we should also point out that the method presented by this paper, as

the traditional single-scale kriging method, is mainly suitable for processing the geochemical

data that follow a normal distribution or log-normal distribution.

Illustrative Examples

In this section, we first demonstrate the validity of the proposed method for estimating

parameter fields at different scales by using several synthetic examples, and then the method

is applied to the vanadium geochemical data measured from stream sediment samples in

Zhejiang Province, China.

Synthetic Examples

In each of following examples, we generate a random field at a finest scale, given

statistics (mean, variance, and correlation lengths) of the field. By local averaging, we derive

fields at different coarse scales, and consider these fields as "true" fields. We then take a

number of samples at these scales. Using these samples, we estimate the kriged fields and

their corresponding conditional covariance at different scales and compare these kriged fields

to the "true" fields to assess the performance of the multiscale kriging method.

In the first example, we consider a one-dimensional column of length 256 (at any

consistent unit), discretized into 256 grid of size 1. The reason we choose this

one-dimensional problem is that the effect of adding conditional points at different scales can

be easily illustrated. A random field with zero mean, unit variance, and separately, isotropic

exponential covariance function of a correlation length 20 is generated at this grid, using the

Karhunen-Loève decomposition method [*Zhang and Lu*, 2004]. This field is taken as the true

field at this finest scale (S_1). At any coarse scale, the true field is computed from the finest scale using Equation (4). We calculate the "true" fields at two coarse scales, at $\Delta x = 2$ (S_2) and $\Delta x = 4$ (S_3), which correspond to grids of 128 and 64, respectively. All these three "true" fields will be used to assess the accuracy of the kriged fields.

We then take $N_1 = 16$ (fine-scale set) and $N_3 = 4$ (coarse-scale set) samples at scales S_1 and S_3, respectively. The locations of the fine-scale samples are marked in Figure 3 as triangles below the horizontal axis, and the locations of the coarse-scale samples in the top of each diagram as inverted triangles. There is no data at the intermediate scale S_2. Our purpose is to estimate the conditional mean and conditional covariance of the field at all three scales S_1, S_2, and S_3.

The estimated mean fields at three different scales are illustrated in Figure 3. Figure 3A compares the finest scale true field (256 grids, red curves) and the estimated field created by the single-scale kriging method using the fine-scale measurements alone (green curve) as well as the estimated field obtained by the multi-scale kriging model using both coarse- and fine-scale measurements (blue curve). It is seen from the figure that, although the estimate using the fine-scale measurements alone captures the general trend of the true field, incorporating coarse-scale measurements does improves the estimate locally. The range of influence of the coarse-scale measurements depends on the correlation length of the original unconditional fields. In the regions that are far away from the coarse-scale measurements, these measurements do not have a significant impact on estimates. In addition, at this finest scale, the estimate using multiscale measurements (blue curve) honors the fine scale measurements, but it does not honor the coarse-scale measurements. The estimation errors using different sets of data can be measured using the root-mean-squared error (RMSE). The

RMSE is reduced from 0.746 for the kriged field using the fine-scale measurements only to 0.686 using both the fine- and coarse-scale measurements.

Figure 3B shows that at the coarse scale (64 grids) the kriged field obtained from the single-scale kriging method using the coarse-scale measurements alone (the green curve) also captures the general trend of the true field (red curves) and honors the measurements at this scale, but it is relatively smooth and does not provide detailed variability of the field. By incorporating the fine-scale measurements with the multiscale kriging model, the estimate has been significantly improved (blue curve). The RMSE is reduced from 0.754 for the kriged field using the coarse-scale measurements alone to 0.601 using both the fine- and coarse-scale measurements. Note that the estimate at the coarse scale in general will not honor the fine-scale measurements.

It should be pointed out that, although the blue curves in Figures 3A and 3B are kriged fields obtained by the multiscale kriging model using both coarse- and fine-scale measurements, these two fields differs slightly, because they represent the conditional mean fields at two different scales.

Figure 3C illustrates the kriging estimates using all measurements for the scale $\Delta x = 2$, at which there is no measurement at all. In general, both coarse- and fine-scale measurement are not honored at this scale. However, it is seen that the estimated field created by multiscale kriging model is reasonably close to the true field at this scale.

Figure 4 depicts the conditional variance of estimated fields at three different scales. At the fine scale, as shown in Figure 4A, using the measurements at this scale alone reduces the conditional variance significantly, especially near the measurement locations, where the

conditional variance is zero (see red curve). Conditional variance is further reduced once the coarse-scale measurements are taken into account (blue curve). Although the conditional variance at the coarse-scale measurement locations has been significant reduced, the variance is not exactly zero, because knowing a value at a location at the coarse scale is not enough to infer the exact value at the same location at the fine scale. The same is true at the coarse scale, as illustrated in Figure 4B. At this coarse scale, the conditional variance at the fine-scale measurement locations is not zero, though it is very small (blue curve). At scale S_2, where there is no measurement available, the conditional variance is not zero at all coarse- or fine-scale measurement locations (Fig. 4C), but the conditional variance at this scale has been significantly reduced, as compared to the unconditional variance of $\sigma_Y^2 = 0.951$ at this scale.

In the second case, we consider a two-dimensional domain of 128×128, discretized into 1×1 elements (scale S_1, 16384 elements in total). A random field with zero mean, unit variance, and an isotropic separable exponential covariance function of correlation length $\lambda = 20$ is generated using the Karhunen-Loève decomposition method [*Zhang and Lu*, 2004]. From this field, two additional fields of grids 64×64 (scale S_2, $\Delta x = \Delta y = 2$, and 4096 elements) and 32×32 (scale S_3, $\Delta x = \Delta y = 4$, and 1024 elements) are derived using Equation (10). These three fields are considered as "true" fields. Suppose that $N_1 = 50$ measurements are taken from fine scale S_1, $N_3 = 10$ measurements from coarse scale S_3, and no observation is available at the intermediate scale S_2. The locations of these measurements are displayed in Figure 5.

Figure 6 compares the true field at the finest scale (Fig. 6A) with the kriged field obtained from the single-scale kriging method using the fine-scale measurements alone (Fig.

6B) and the kriged field created by the multiscale kriging model using measurements at both fine and coarse scales (Fig. 6C). The figure shows that the kriged field using the fine-scale measurements alone captures the most of the heterogeneities of the true field but incorporating additional measurements at the coarse scale using the multiscale-kriging method improves the accuracy of the estimated field slightly. The root mean square error of the kriged fields is reduced from 0.750 for the estimated field using the fine-scale measurements to 0.684 for the field estimated using measurements at both the fine and coarse scales.

Figure 7 illustrates the comparison between the fields of the conditional variance at the fine scale, conditioned at fine-scale measurements only (Fig. 7A) and at both fine- and coarse-scale measurements (Fig. 7B). A significant reduction of the local conditional variance is evident around the coarse-scale conditioning points by incorporating coarse-scale measurements in estimating the fine-scale field.

At the coarse scale, since only a small number of measurements are available, the kriged field using these coarse-scale measurements alone is very close to a relatively uniform, unconditional mean field, as illustrated in Figure 8B. However, if the fine-scale measurements are also incorporated into the kriged field, it becomes much close to the true field (Fig. 8C). The root mean square error of the kriged fields at the coarse scale is reduced from 0.865 for the estimated field using the coarse-scale measurements to 0.619 for the field estimated using measurements at both the fine and coarse scales.

It should be noted again that the fields presented in Figures 6C and 8C are slightly different, even though both of them are kriged fields using all fine- and coarse-scale

measurements. These two fields represent conditional fields at two different scales.

Figure 9 compares the conditional variance at the coarse scale, using coarse-scale measurements alone (Fig. 9A) and using all coarse- and fine-scale measurements (Fig. 9B). The figure demonstrates that incorporating fine-scale measurements significantly reduces the conditional variance at the coarse scale.

At the intermediate scale, where there is no data available, the conditional mean and variance can be estimated from measurements at other scales. Figure 10 compares the true field at this scale (Fig. 10A) against the estimated conditional mean field using measurements at both fine and coarse scales (Fig. 10B). Figure 11 illustrates the conditional variance at this intermediate scale by using measurements at other two scales. It is seen from these figures that the conditional mean field estimated using measurements at other scales is close to the true field and that the conditional variance can be significantly reduced. This example demonstrates that this multiscale simple kriging method can be used to estimate the conditional mean and variance fields at any scale where there is no data available, as long as measurements are available at some other scales.

Application to Geochemical Surveyed Data

In the previous discussion, our method has been tested on several synthetic examples in general. Here, the vanadium (V) geochemical data measured from 8402 stream sediment samples in Zhejiang Province, China, are used to further demonstrate the validity of the multiscale kriging method. These stream sediment data are supplied by the Zhejiang Geophysical and Geochemical Exploration Institute. The samples were collected at the mouth of first-order streams or in the connected second-order stream in 1980−1986. Figure 12 shows

the spatial distribution of the total 8402 sample stations (in the figure, 14641 meshes in total, of which 6239 meshes are empty). At each sampling station, sediment was gathered at four points with an average sampling density of 1 point /1 km^2. Samples from each station were composed of an equal weight of sediment from these four sampling points. The minimum weight of each sample is 2.5kg. The composite samples from these stations, with an average density of one sample per 4 km^2 , were submitted to the laboratory for chemical analysis. The content of vanadium was determined by the X-ray fluorescence spectrometry analysis with the detection limit of 15 ppm. Figure 13 illustrates the result obtained for the V data as a histogram and "Probability–Probability" plot (P–P plot). It is shown that these V content measurements follow a normal distribution.

We consider these original measured data (contrast set) on the grid of 2×2-km (one sample per 4 km^2) as the spatially distributed dataset at the finest scale, from which the vanadium content at two additional coarser scales of 8×8-km (Set A, 3660 meshes, 2084 measured samples in total) and16×16-km (Set B, 915 meshes, 524 measured samples in total) are derived. Because of space limit, we here only discuss the comparison of the conditional variance for a one-dimensional column A'_1—A'_{121} of length 121 as indicated in Figure 12. It is seen from Figure 14 that the conditional variance of the estimated field created by the multiscale Kriging method using both Sets A and B (green curve) is obviously smaller than that of single-scale Kriging method alone using Set A (red curve), because more information (Set B) has been used in the multiscale kriging. Since the traditional simple kriging cannot be applied to the case of multiscale data points, to make our comparisons more reasonable, we map set B (which is on the 16×16-km support scale) onto the support scale of 8×8-km and

combine the resulted dataset with set A (which is also on 8×8-km) to form the dataset C (3660 meshes, of which 2608 meshes have samples). The conditional variance from the simple kriging using this combined dataset C is also compared with the conditional variance from the multiscale kriging method using Sets A and B. The figure indicates that, using the same dataset, the multiscale kriging method may produce more accurate results than the single-scale kriging method, even though the same set of measurements is used (comparing green and blue curves). The reason is that, if multi-scale data are available, the multiscale kriging effectively take the scale information into account, while in the single-scale kriging, such scale information has been lost.

Summary and Conclusions

In this study, we propose a simple multiscale kriging algorithm to incorporate data observed at multiscales (multi-resolutions). We assume that there are a number of measurements at different scales that may be different from the target scale at which the parameter values are needed. Similar to the simple kriging, the parameter at the target scale is represented as a linear combination of all available measurements and the coefficients in this linear combination are solved from the kriging system, which is related to covariance functions across the scales. The key point in this method is to find the covariance functions between blocks at different scales. We illustrated the method using several one-dimensional and two-dimensional synthetic examples as well as measured geochemical data.

These examples demonstrate that, at any scale at which some measurements are available, by incorporating measurements from all scales, the estimated field is better than the field estimated only using the measurements at this scale.

Second, if measurements are available at the target scale, these measurements will be honored. However, measurements at other scales will not be honored at the target scale, even though they will reduce the conditional covariance at the target scale.

Furthermore, this method allows us to estimate a parameter field at the scale that does not have any measurements. In this case, the conditional mean field and conditional covariance can be found using measurements at other scales. Of course, all measurements will not be honored at the target scale. The method may be useful in some applications, such as numerical adaptive mesh refinement.

Acknowledgements

REFERENCES

Clark, I., Practical Geostatistics, Applied Science Publishers, 1979.

Deutsch, C. V., and Journel A. G., GSLIB, Geostatistical Software Library and User's Guide, Second Edition, Oxford University Press, 1998.

Journel, A. G. and Huijbregts C., Mining Geostatistics, Academic Press, 1978.

Kitanidis, P. K., Introduction to Geostatistics, Applications in Hydrogeology, Cambridge University Press, 1997.

Kupfersberger, H., Deutsch, C. V., Journel, A. G., Deriving constraints on small-scale variograms due to variograms of large- scale data, Math. Gol., 30(7), 837-852, 1998.

Vanmarcke, E, Random fields: Analysis and Synthesis, The MIT Press, 1983.

Zhang, D. and Lu, Z. , An efficient, higher-order perturbation approach for flow in randomly heterogeneous porous media via Karhunen-Loève decomposition, J. of Comput. Phys., 194(2), 773-794, 2004.

Zhao, P. (eds), Quantitative Geoscience: Methods and its applications. Higher Education Press, Beijing, 2004.

Figure Captions

Figure 1 Schematic diagram defining various distances characterizing the relative positions of two segments.

Figure 2 Schematic diagram defining various distances characterizing the relative positions of two rectangular blocks.

Figure 3 Comparison of the one-dimensional true fields and kriged mean fields at three scales: (A) fine scale, (B) coarse scale, and (C) the intermediate scale at which no measurements are available. Triangles below the horizontal axis show the locations of the fine-scale samples, and inverted triangles along the upper horizontal axis depict the locations of the coarse-scale samples (see the text).

Figure 4 Comparison of the conditional variance for the one-dimensional case computed using different sets of data at three scales: (A) fine scale, (B) coarse scale, and (C) the intermediate scale at which no measurements are available. Triangles below the horizontal axis show the locations of the fine-scale samples, and inverted triangles along the upper horizontal axis depict the locations of the coarse-scale samples(see the text).

Figure 5 Locations of conditioning points in the two dimensional example with $N_1 = 50$ (circles) and $N_3 = 10$ (squares).

Figure 6 Comparison of the true field (A), and the kriged mean fields using fine-scale data (B), and multiscale data (C), at the two-dimensional fine scale.

Figure 7 Conditional variance at the fine scale, computed using fine-scale data only (A), and multiscale data (B).

Figure 8 Comparison of the true field (A), and the kriged mean fields using fine-scale data (B)

and multiscale data (C), at the coarse scale.

Figure 9 Conditional variance at the coarse scale, computed using fine-scale data only (A), and multiscale data (B).

Figure 10 Comparison of the true field (A), and the kriged field using multiscale data (B), at the intermediate scale where no measurements are available.

Figure 11 Conditional variance at the intermediate scale using multiscale data.

Figure 12 Locations of stations sampling stream sediments in Zhejiang Province, China.

Figure 13 Histogram and P–P plot for the vanadium content in stream sediments (8402 samples) from Zhejiang Province: (a) histogram; and (b) P–P plot.

Figure 14 Comparison of the conditional variance for the one-dimensional case computed using different sets of vanadium geochemical data measured from stream sediments.
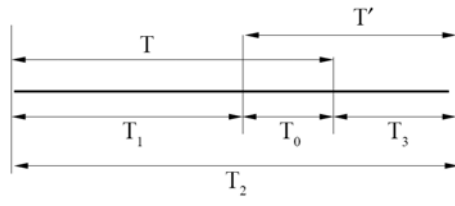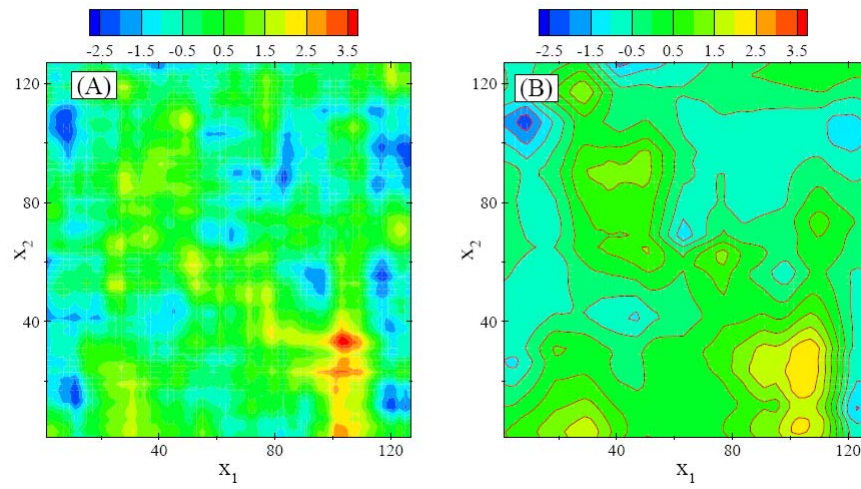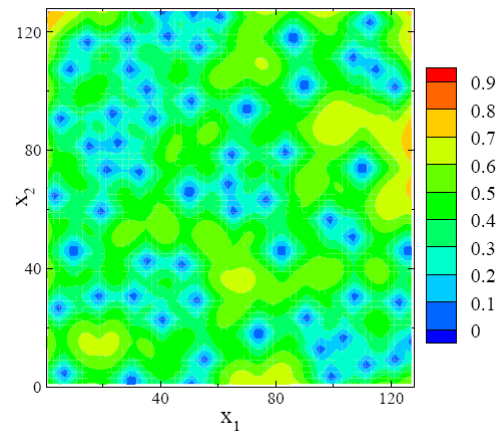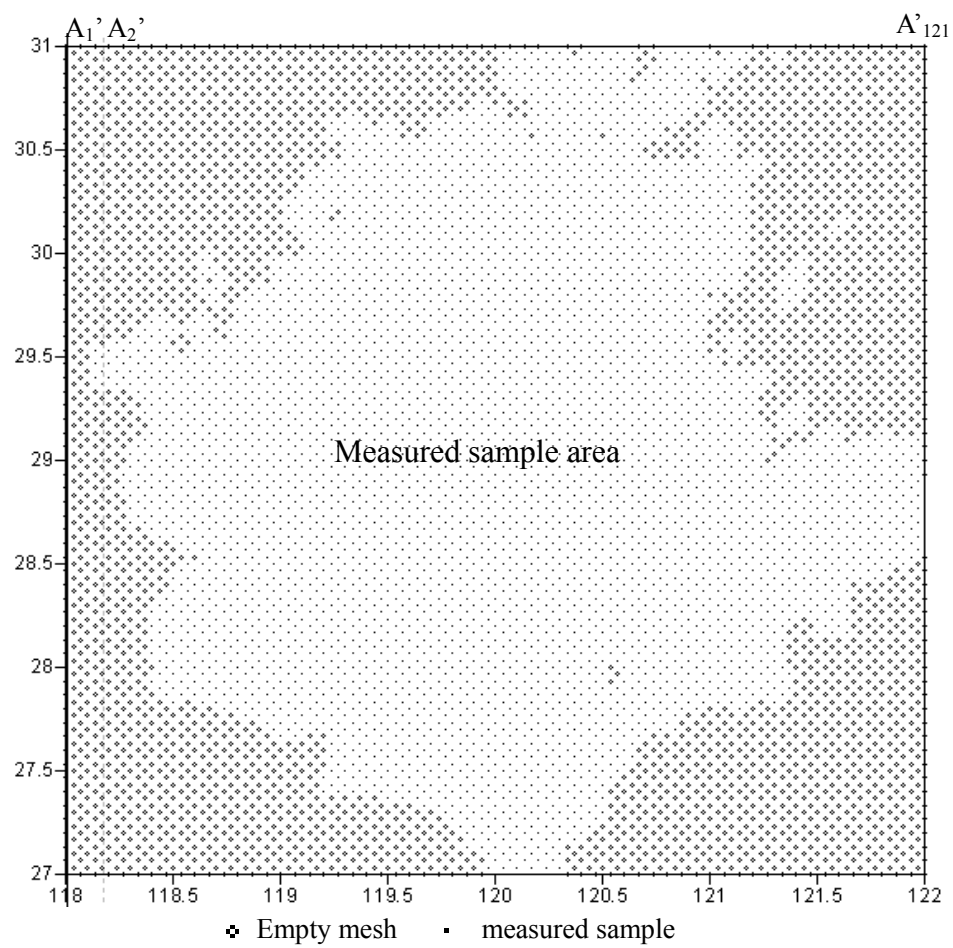
Figure 1
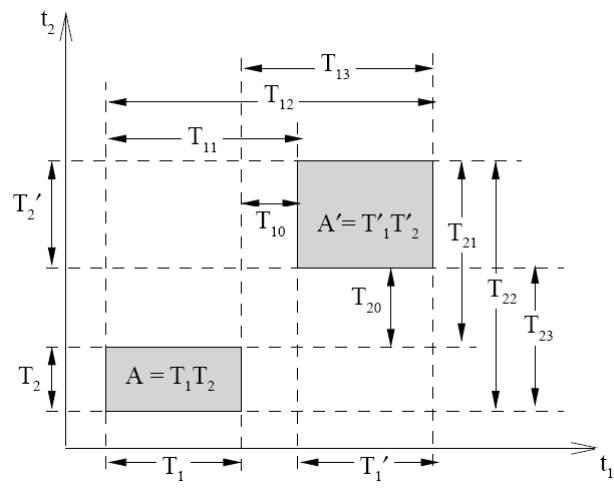
Figure 2
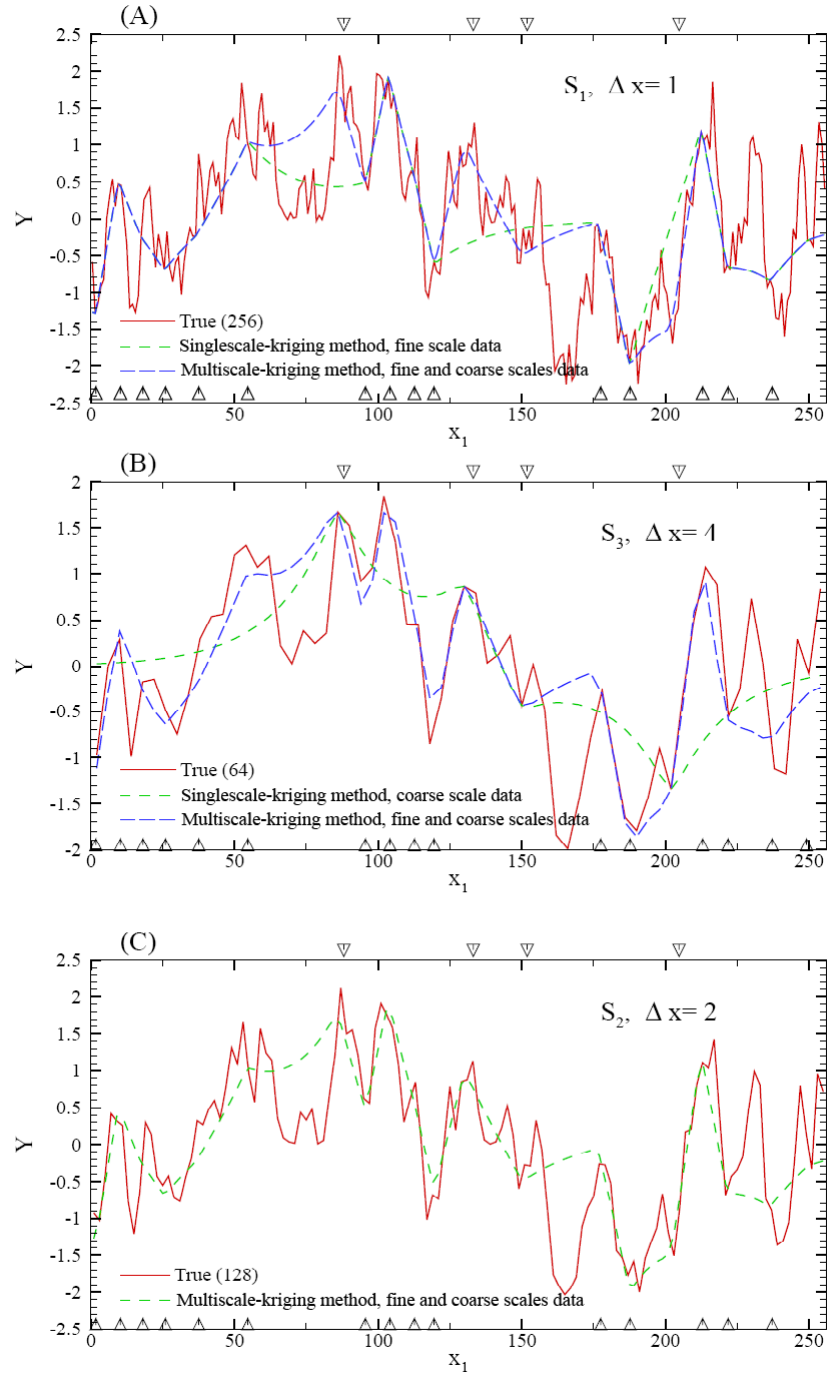
Figure 3
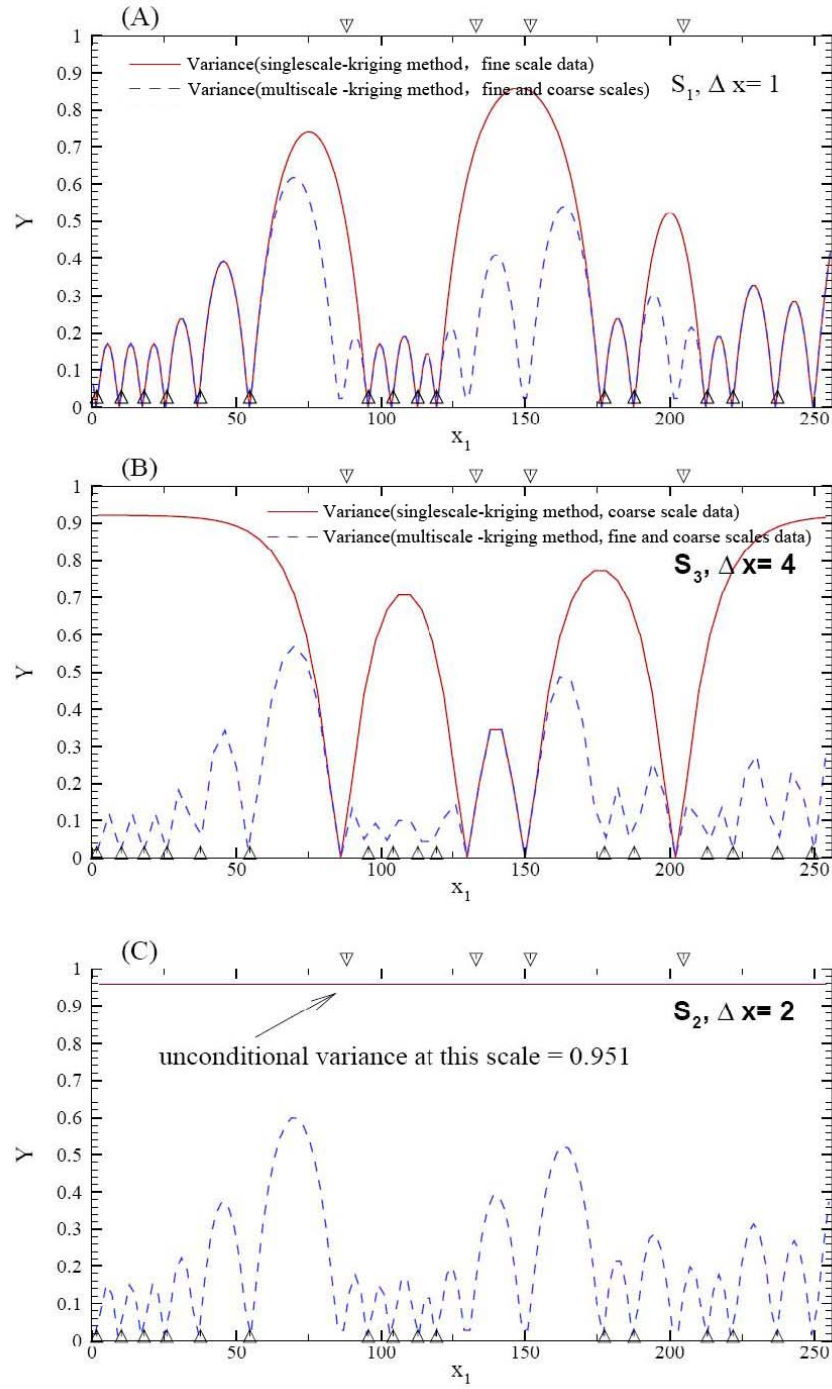
Figure 4
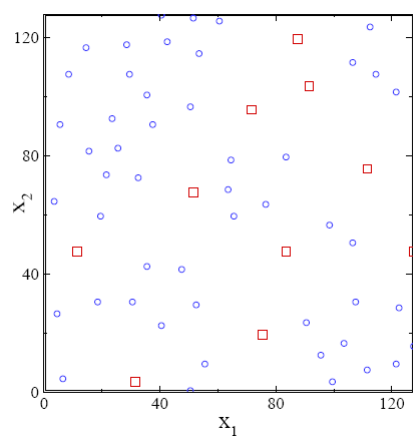
Figure 5
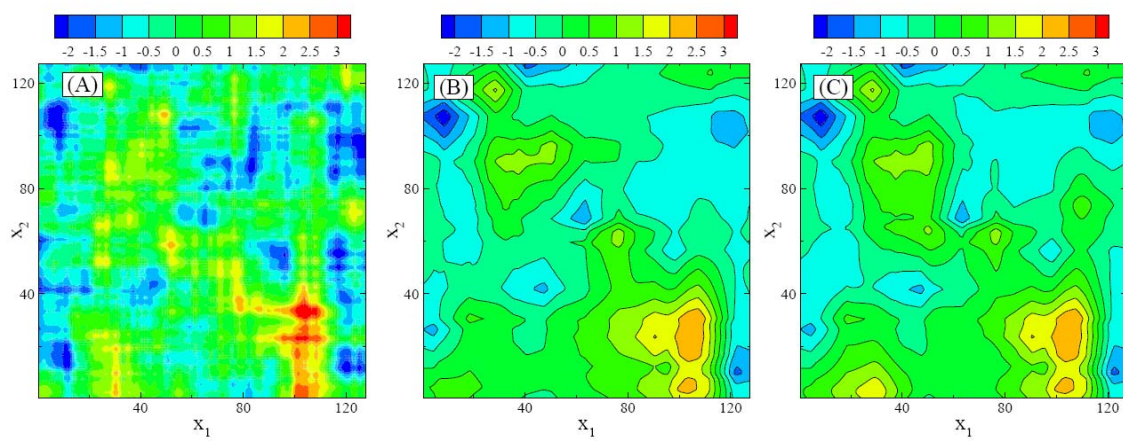
Figure 6
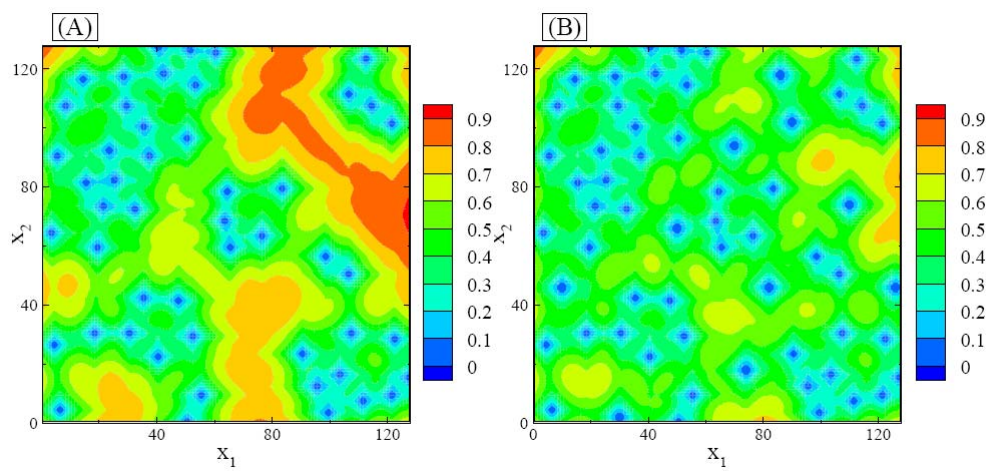
Figure 7
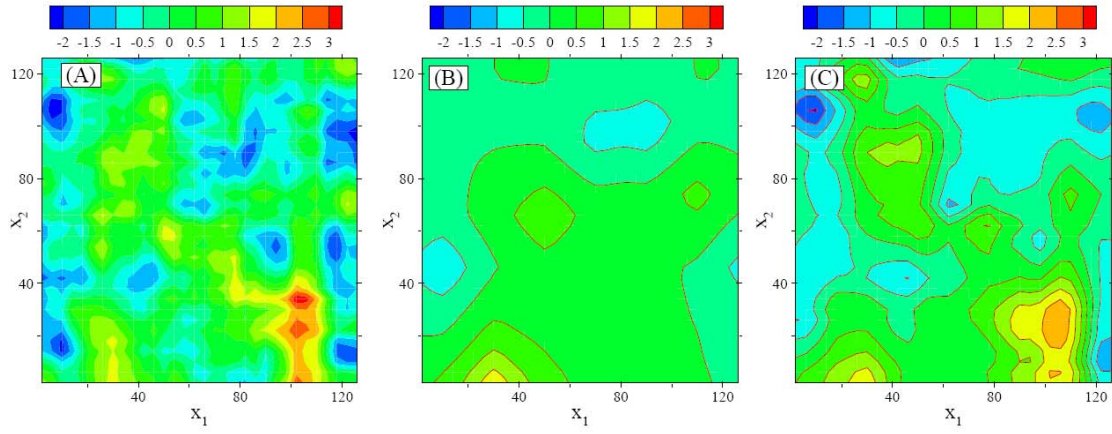
Figure 8
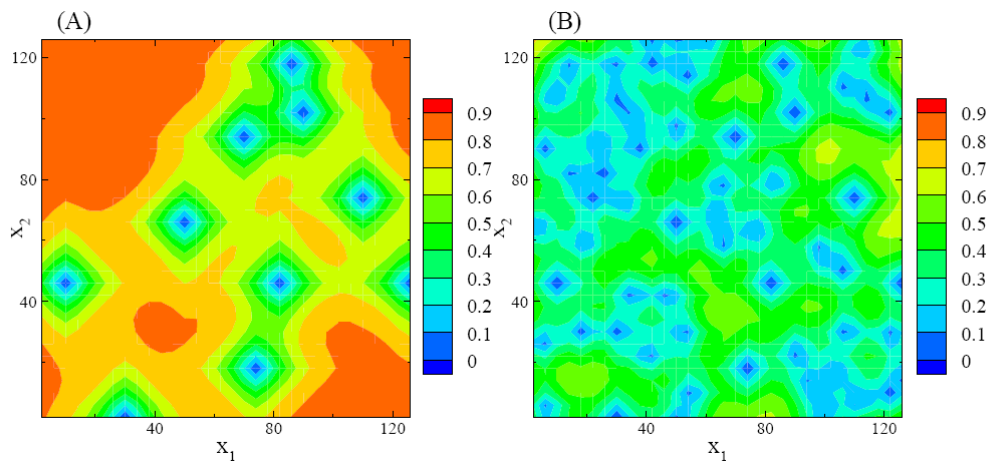
Figure 9

Figure 10

Figure 11

Figure 12

(a)

N = 8402
Mean = 66.75
Minimum = 14.12
Maximun = 331.60
Variance = 911.11
Std.Dev =30.18

(b)

Figure 13

Figure 14